

Physical properties of $\text{La}_{0.67}\text{Ca}_{0.13}\text{Sr}_{0.2}\text{Mn}_{1-x}\text{Fe}_x\text{O}_3$ compounds doped Fe

F.S. Shokr*, M. Hussein

Physics Department, Rabigh College of Science and Arts, P.O. Box 344, Rabigh, 21911, King Abdulaziz University, Jeddah, Saudi Arabia



ARTICLE INFO

Article history:

Received 6 August 2017

Received in revised form 29 October 2017

Accepted 5 November 2017

Available online 8 November 2017

Keywords:

Magnetism

X-ray diffraction

Transport electric properties

Mössbauer spectrometry

ABSTRACT

$\text{La}_{0.67}\text{Ca}_{0.13}\text{Sr}_{0.2}\text{Mn}_{1-x}\text{Fe}_x\text{O}_3$ ($x = 0-0.1$) compounds were synthesised by standard sol-gel reaction and characterised by X-ray diffraction at room temperature. X-ray diffraction and Rietveld refinement show that they crystallize in the rhombohedral structure with the $R\bar{3}c$ space group. The magnetic behavior (magnetization and Curie temperature T_C) shows a large dependence on the fractional composition x . The Mössbauer results reveal the presence of iron ion at the trivalent state Fe^{3+} assigned by the same isomer shift δ value. Resistivity measurements, performed between 10 and 350 K, show a metal–insulator transition for $0.0 \leq x < 0.1$ and a pure insulator behavior for $x = 0.1$.

The suppression of metallic behavior and ferromagnetism under the doping effects of Fe will be discussed in terms of doping disorder, Fe–Mn super-exchange interactions and a site percolation mechanism.

© 2017 Published by Elsevier B.V. This is an open access article under the CC BY-NC-ND license (<http://creativecommons.org/licenses/by-nc-nd/4.0/>).

Introduction

For twenty years, researchers worldwide have given a great interest in mixed valence manganites $\text{Ln}_{1-x}\text{A}_x\text{MnO}_3$ -type (where Ln is a lanthanide cation and A is usually an alkaline earth ion) due to the colossal magnetoresistance (CMR) and the magnetocaloric properties displayed by some compounds of this family [1–5]. On one hand, films [6] of these materials have potential applications, e.g. as magnetic sensors or in computer memory system. On the other hand, it is expected that the understanding of the underlying physical mechanisms could lead to substantial advances in the field of strongly correlated electron physics. The conventional understanding of electrical transport and magnetic properties is generally based on the double exchange (DE) mechanism [7], which considers the ferromagnetic (FM) coupling and the e_g electrons hopping through $\text{Mn}^{3+}-\text{O}^{2-}-\text{Mn}^{4+}$ bond. However, theoretical considerations indicate that the DE mechanism alone could not quantitatively account for all the physics in these compounds. The Jahn–Teller distortions, lattice, spin and orbital degrees of freedom should be considered [8,9].

Many previous studies have been reported on the effects of Mn site substitution by foreign elements in $\text{La}_{0.7}(\text{Ca}, \text{Sr})_{0.3}\text{MnO}_3$ such as Ga [10], Al [11], Co [12], Ti [13], Cr [14–19], etc. . . Generally, doping at Mn site decreases the Curie temperature (T_C) and the metal–insulator (M-I) electric transition temperature (T_p). These studies

allow authors to discuss the influence of Fe doping on the structural, magnetic and electrical transport properties.

This paper is intended to obtain characterization of the $\text{La}_{0.70}\text{Ca}_{0.15}\text{Sr}_{0.15}\text{Mn}_{1-x}\text{Fe}_x\text{O}_3$ system, including the novel results of conductivity measurement. The systematic investigations of all the structural, magnetic and transport properties were performed on the same and well defined samples.

Experimental

The $\text{La}_{0.70}\text{Ca}_{0.15}\text{Sr}_{0.15}\text{Mn}_{1-x}\text{Fe}_x\text{O}_3$ ($x = 0.000, 0.025, 0.050, 0.075$ and 0.100) compounds were synthesized using the sol-gel method as described in reference [20]. The final heat treatment was performed at 1200 °C for 24 h. The X-ray diffraction patterns were recorded on a PHILIPS X'PERT diffractometer using $\text{Co K}\alpha$ radiation. The analysis of the phase was carried out by the FULLPROF program based on the Rietveld method [21]. The Mössbauer measurements were performed at room temperature using transmission Mössbauer spectrometry. The ^{57}Co (Rh) source was mounted on a constant acceleration triangular motion velocity transducer. The values of isomer shift are referred to that of α -Fe absorber at room temperature. The fitting procedure was performed with a current routine based on the least-squares minimization. The hyperfine parameters were determined from the fitted spectra collected at room temperature.

Magnetic measurements were performed in BS1 and BS2 magnetometer developed in Louis Néel Laboratory of Grenoble. The magnetization curves were obtained under an applied magnetic

* Corresponding author.

E-mail address: drf.shokr@outlook.com (F.S. Shokr).

field ranging from 0 to 5 T at temperatures ranging from 100 to 400 K. Finally, the electrical resistance was measured by the four probe technique, developed in MCMF Laboratory of Grenoble, using current at most 10 mA.

Results and discussions

The Crystalline structure determination of our samples was obtained from X-ray diffraction analysis.

X-ray diffraction patterns for $\text{La}_{0.7}\text{Ca}_{0.15}\text{Sr}_{0.15}\text{Mn}_{1-x}\text{Fe}_x\text{O}_3$ ($x = 0-0.1$) compounds are reported in Fig. 1. They give evidence that all samples are single phased. We state that some doublets, present for $x = 0$, disappear after Fe-doping. Despite this change in XRD pattern, no significant structural transition is detected, hence all compounds can be indexed in the rhombohedral structure with $R\bar{3}c$ space group as we can see in Fig. 2, for $x = 0.025$ and 0.075 .

The results of XRD patterns refinements, based on Fullprof program, are gathered in Table 1. R_p Residuals pattern, R_F structure factor and χ^2 goodness of fit are listed as well. In addition, V unit

Table 1

Lattice parameters and cell volume of $\text{La}_{0.7}\text{Ca}_{0.15}\text{Sr}_{0.15}\text{Mn}_{1-x}\text{Fe}_x\text{O}_3$ compounds.

x	0.000	0.025	0.050	0.075	0.100
Space group	$R\bar{3}c$	$oR\bar{3}c$	$R\bar{3}c$	$R\bar{3}c$	$R\bar{3}c$
$\langle r_A \rangle$ (Å)	1.22(4)	1.22(4)	1.22(4)	1.22(4)	1.22(4)
$\langle r_B \rangle$ (Å)	0.70(4)	0.70(4)	0.70(4)	0.70(4)	0.70(4)
a_r (Å)	5.15(8)	5.47(1)	5.47(1)	5.47(8)	5.47(8)
α (°)	60.48(1)	60.25(5)	60.27(6)	60.13(8)	60.19(2)
V (Å ³)	57.78(1)	58.22(2)	58.25(3)	58.32(5)	58.38(1)
Mn/Fe(site b)					
x	0.0000	0.0000	0.0000	0.0000	0.0000
y	0.0000	0.0000	0.0000	0.0000	0.0000
z	0.0000	0.0000	0.0000	0.0000	0.0000
La,Ca,Sr (site a)					
x	0.0000	0.0000	0.0000	0.0000	0.0000
y	0.0000	0.0000	0.0000	0.0000	0.0000
z	0.2500	0.2500	0.2500	0.2500	0.2500
O (site e)					
x	0.4470	0.5554	0.5423	0.5483	0.5412
y	0.0000	0.0000	0.0000	0.0000	0.0000
z	0.2500	0.2500	0.2500	0.2500	0.2500
Mn-O	1.95(2)	1.95(1)	1.95(2)	1.95(7)	1.95(2)
Mn-O-Mn	162.89(1)	162.16(4)	166.33(4)	164.43(5)	166.69(5)
R_p	16.0	23.2	32.6	29.4	28.3
R_F	6.49	5.56	15.0	7.83	14.1
χ^2	2.26(4)	1.60(4)	1.60(3)	1.73(3)	2.95(8)

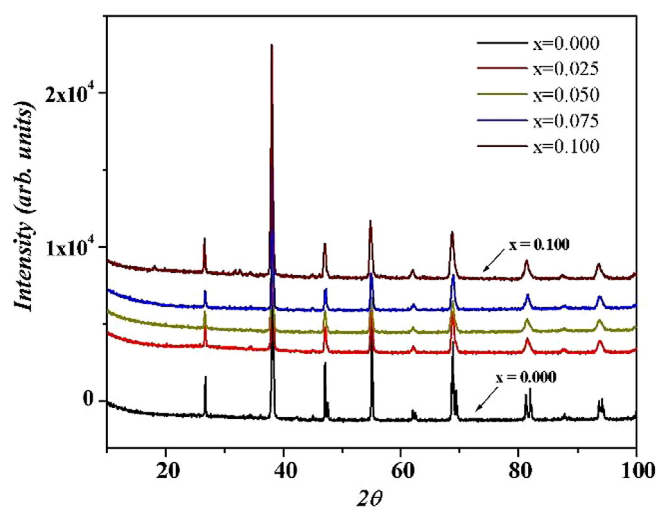


Fig. 1. X-ray diffraction patterns of $\text{La}_{0.7}\text{Ca}_{0.15}\text{Sr}_{0.15}\text{Mn}_{1-x}\text{Fe}_x\text{O}_3$ ($x = 0.00, 0.025, 0.050, 0.075$ and $x = 0.100$) compounds.

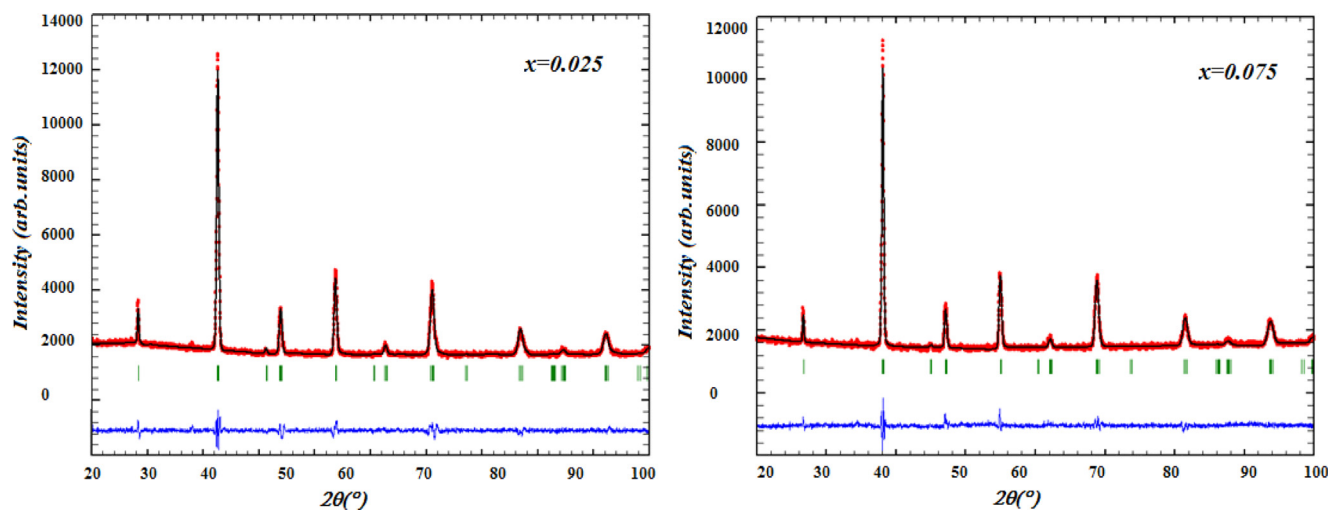


Fig. 2. Observed (solid circles) and calculated (solid line) XRD patterns of the Fe-doped samples ($x = 0.025$ and 0.075) obtained at room temperature. The difference between these spectra is plotted at the bottom. Bragg reflections are indicated by ticks. (For interpretation of the references to colour in this figure legend, the reader is referred to the web version of this article.)

cell volume, Mn–O average bond length and Mn–O–Mn average bond angles values are added in the same table. As main conclusion from these results, no significant structural change for $\text{La}_{0.7}\text{Ca}_{0.15}\text{Sr}_{0.15}\text{Mn}_{1-x}\text{Fe}_x\text{O}_3$ compounds ($0 \leq x \leq 0.1$) is observed.

The zero-field Mossbauer spectra at room temperature of the two samples ($x = 0.075$ and 0.100) are shown in Fig. 3. The spectra present the similar profiles and the presence of a single Mossbauer paramagnetic doublet with different quadruples splitting (ΔE_Q) is evidenced. We have fitted both spectra with a single quadruple split doublet and the resulting hyperfine parameters are given in Table 2. Taking into account the calculation errors, both spectra have the same isomer shift δ value which is assigned to Fe^{3+} . We can mention that the ΔE_Q value increases versus Fe-doping content.

The temperature dependence of the magnetization measurements M (T), under applied magnetic field of 0.05 T, reveals a

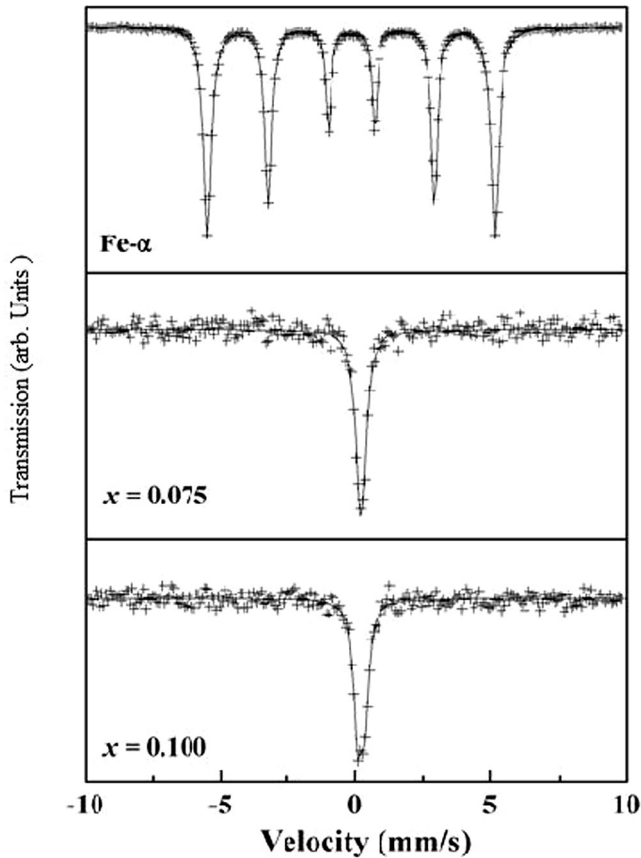


Fig. 3. Mössbauer spectra collected at room temperature of $\text{La}_{0.7}\text{Ca}_{0.15}\text{Sr}_{0.15}\text{Mn}_{1-x}\text{Fe}_x\text{O}_3$ ($x = 0.075$ and $x = 0.1$) compounds.

Table 2

Estimated parameters from the Mössbauer spectra of $\text{La}_{0.7}\text{Ca}_{0.15}\text{Sr}_{0.15}\text{Mn}_{1-x}\text{Fe}_x\text{O}_3$ ($x = 0.075$ and 0.100) compounds.

x	δ (mm/s)	ΔE_Q (mm/s)
0.075	0.35	0.08
0.100	0.36	0.24

ferromagnetic–paramagnetic transition for all samples (Fig. 4). The transition occurs at Curie temperature (T_C), where dM/dT shows a minimum. The iron introduction in the Mn site causes, as expected, a significant decrease in the temperature of ferromagnetic ordering (T_C) [22]. This result has explained by Othmani et al. [20], as a positive contribution of the double exchange mechanism due to the Fe presence. This effect is also reported in the electrical transport properties.

The resistivity temperature dependences of $\text{La}_{0.7}\text{Ca}_{0.15}\text{Sr}_{0.15}\text{Mn}_{1-x}\text{Fe}_x\text{O}_3$ ($x = 0-0.1$) compounds are displayed in Fig. 5. For $x < 0.1$, all samples undergo a typical metal–insulator transition at T_p temperature, corresponding to the maximum of resistivity. Resistivity increase accompanied by T_p decrease versus Fe content is observed as well. A similar behavior was observed in Cr-substituted manganites by Kallal et al. [23]. The resistivity increase is essentially due to the disorder introduced in the charge transfer mechanism when replacing some links of the $\text{Mn}^{3+}-\text{O}^{2-}-\text{Mn}^{4+}$ bond by $\text{Mn}^{3+}-\text{O}^{2-}-\text{Fe}^{3+}$. When x reaches 0.100, the compound has an insulator behavior over the entire temperature range, upper to 100 K.

The transport in manganites is closely related to the spin of the e_g carriers and the localized t_{2g} spin core in Mn^{3+} ions. This is

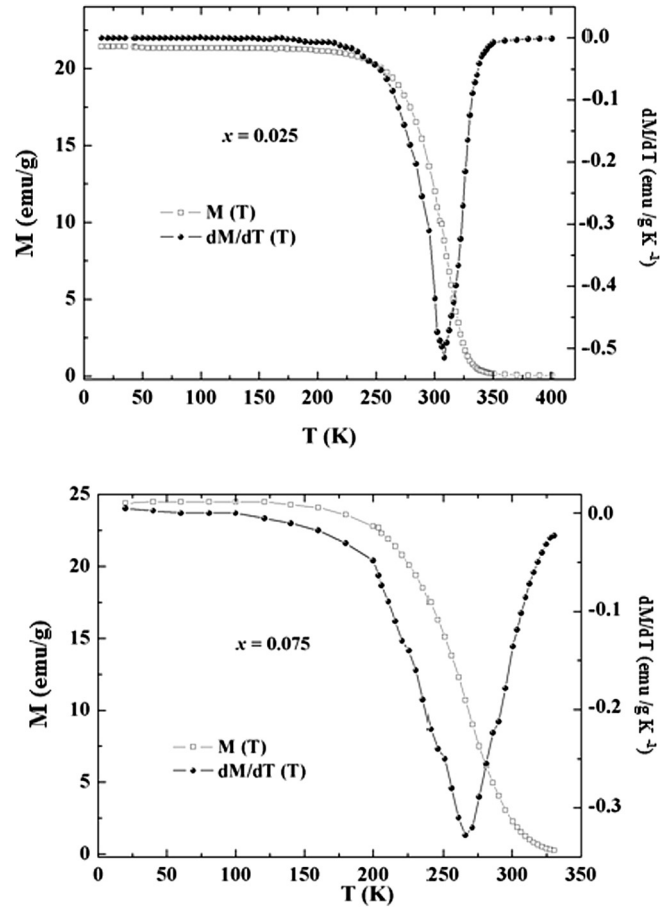


Fig. 4. Temperature dependence of the magnetization (M) and (dM/dT) for $x = 0.025$ and 0.075 samples.

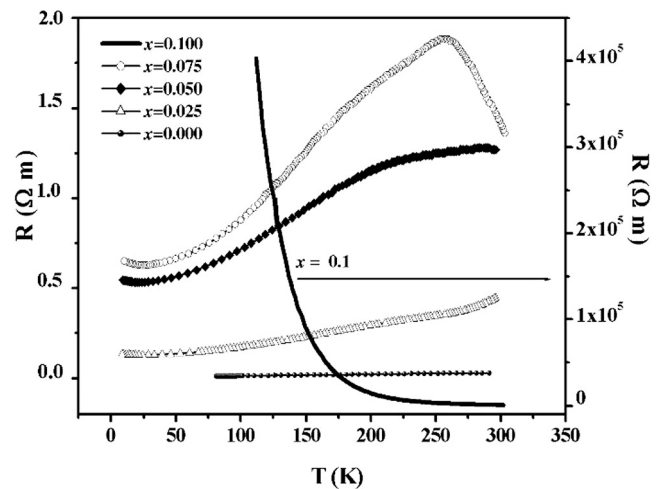


Fig. 5. Temperature dependence of the resistivity of the $\text{La}_{0.7}\text{Ca}_{0.15}\text{Sr}_{0.15}\text{Mn}_{1-x}\text{Fe}_x\text{O}_3$ ($x = 0.000, 0.025, 0.050, 0.075$ and 0.100) compounds.

explained by the double exchange model and Jahn–Teller lattice distortion. At $T < T_p$, the double exchange interaction becomes stronger. According to Pauli Exclusion Principle, only when the spin direction of the jumping e_g electrons is identical with that of the acceptor Mn^{4+} ions, the $2p$ electrons of the O^{2-} ions satisfy Hund's rule. The e_g electrons of the Mn^{3+} ions jump more easily

between the Mn^{3+} and Mn^{4+} ions through the O^{2-} ions. By the substituting of the Fe at Mn site, Xavier et al. [24] report that the Fe clusters depolarize the spins of their Mn neighbors leading to the decrease of the conduction by scattering off these depolarized spins in this doping regime. Rao et al. [25] have proposed a phenomenological cluster model. It is known that the top of the Fe e_g band is near the bottom of the Mn e_g band. The substituted Fe ions act as trapping centers for the e_g electrons and as result reduce the hopping of the e_g electrons between the Mn^{3+} and Mn^{4+} ions. So, we can deduce that these trapping centers perturb the double exchange interaction and leading to an increase of the resistivity. The T_p value is mainly dependent on the lattice distortion, the ratio of the Mn^{3+}/Mn^{4+} ions and the oxygen deficiency [26]. The samples preparation conditions are identical and thereby these samples have the same oxygen deficiency. So we can consider that this parameter is negligible in comparing the T_p . The difference of the atomic radius between the A–O layer and Mn–O layer leads to the mismatch of the adjacent atomic layers. This creates distortion and results in the change of the bond angles from 180° of the ideal cubic structure in $AMnO_3$ to less than 180° . The octahedron is tilted and shows the alternating buckling with the tolerance factor. If the distortion is stronger, the orbits of the itinerant electrons split and the double exchange interaction weakens. Therefore the transfer of the electrons is forbidden and the resistivity increases. When the Mn elements are partially substituted by the Fe elements, the distortion becomes stronger and the double exchange interaction weakens, so the resistivity increases and the T_p shifts to the lower temperatures.

Conclusion

In a summary, a systematic investigation of the structural, magnetic and transport properties in the $La_{0.70}Ca_{0.15}Sr_{0.15}Mn_{1-x}Fe_xO_3$ compounds has been carried out. Rietveld analyses indicate that these samples crystallize in rhombohedral structure with $R\bar{3}c$ space group and the lattice parameters are not affected by iron substitution. Mossbauer spectra pointed, for both compositions ($x = 0.075$ and 0.100), to the same δ isomer shift values close to that of iron Fe^{3+} . The magnetic study revealed a significant decrease in the temperature of ferromagnetic ordering (T_C) when Mn is substituted by Fe. The electrical characterizations show that all samples exhibit a typical metal–insulator transition for $x < 0.100$ and an insulating behavior for $x = 0.100$. Iron ions enter the lattice as trivalent ions to substitute for Mn^{3+} and act as trapping centers for the e_g electrons. This leads to magnetization weakening which results in T_C decrease, resistivity increase and decrease of both T_C and T_p temperatures, corresponding to magnetic and metal–insulator transition respectively.

Acknowledgment

This Project was funded by the Deanship of Scientific Research (DSR) at King Abdulaziz University, Jeddah, under grant no. G-374-665-37. The authors, therefore, acknowledge with thanks the DSR for technical and financial support.

References

- [1] Dhahri N, Dhahri A, Cherif K, Dhahri J, Belmabrouk H, Dhahri E. Effect of Co substitution on magnetocaloric effect in $La_{0.67}Pb_{0.33}Mn_{1-x}Co_xO_3$ ($0.15 \leq x \leq 0.3$). *J Alloys Compd* 2010;507:405.
- [2] Chahara K, Ohno T, Kasai M, Kozono Y. Magnetoresistance in magnetic manganese oxide with intrinsic antiferromagnetic spin structure. *Appl Phys Lett* 1993;63:1990.
- [3] Tozri A, Dhahri E, Hlil EK. Magnetic transition and magnetic entropy $La_{0.8}Pb_{0.1}MnO_3$ and $La_{0.8}Pb_{0.1}Na_{0.1}MnO_3$. *Mater Lett* 2010;64:2138.
- [4] Tokura Y, Urushibara A, Morimoto Y, Arima T, Asamitsu A, Kido G, Furukawa N. Giant magnetotransport phenomena in filling-controlled kondo lattice system: $La_{1-x}Sr_xMnO_3$. *J Phys Soc Jap* 1994;63:3931.
- [5] Dhahri E, Guidara K, Cheikhrouhou A, J.C., Pierrejoubert J. Giant magnetoresistance at room temperature achieved in the ferromagnetic phase of powder $La_{0.5}Sr_{0.5}MnO_3$ (Article). *Phase Trans* 1998;66:99.
- [6] Jin S, Tiefel TH, McCormack M, Fastnacht RA, Ramesh R, Chen LH. Thousandfold change in resistivity in magnetoresistive La–Ca–Mn–O films. *Science* 1994;264:413.
- [7] Zener C. Interaction between the d-Shell in the Transition Metals. II. Ferromagnetic compounds of manganese with Perovskite Structure. *Phy Rev* 1951;82:403.
- [8] Millis AJ, Littlewood PB, Shraiman BI. Double exchange alone does not explain the resistivity of $La_{1-x}Sr_xMnO_3$. *Phys. Rev Lett* 1995;74:5144.
- [9] Abdelmoula N, Dhahri E, Fourati N, Reversat L. Monovalent effects on structural, magnetic and magnetoresistance properties in doped manganite oxides. *J Alloys Compd* 2010;507:405.
- [10] Sun JR, Rao GH, Liang JK, Shen BG, Wong HK. Doping effects arising from Fe and Ge for Mn in $La_{0.7}Ca_{0.3}MnO_3$. *Appl Phys Lett* 1998;73:2998.
- [11] Blasco J, Garcia J, de Teresa JM, Ibarra MR, Perez J, Algarabel PA, Marquina C. Structural, magnetic and transport properties of the giant magnetoresistive perovskites $La_{2/3}Ca_{1/3}Mn_{1-x}Al_xO_{3-\delta}$. *Phys Rev B* 1997;55:8905.
- [12] Song H, Kim W, Kwon SJ. Magnetic and electronic properties of transition-metal-substituted perovskite manganites $La_{0.7}Ca_{0.3}Mn_{0.95}X_{0.05}O_3$ ($X=Fe, Co, Ni$). *J Appl Phys* 2001;89:3398.
- [13] Cao D, Bridges F, Anderson M, Ramirez AP, Olapinski M, Subramanian MA, Booth CH, Kwei GH. Local distortions in $La_{0.7}Ca_{0.3}Mn_{1-y}A_yO_3$ ($A=Ti$ and Ga) colossal magnetoresistance amplex: Correlations with magnetization and evidence for cluster formation. *Phys Rev B* 2001;64:184409.
- [14] Ghosh K, Ogale SB, Ramesh R, Greene RL, Venkatesan T, Gapchup KM, Bathe Ravi, Patil SI. Transition-element doping effects in $La_{0.7}Ca_{0.3}MnO_3$. *Phys Rev B* 1999;59:533.
- [15] Wu BM, Li B, Zhen WH, Ausloos M, Du Y-L, Fagnard JF, Vanderbemden Ph. Spin-cluster effect and lattice-deformation-induced Kondo effect, spin-glass freezing and strong phonon scattering in $La_{0.7}Ca_{0.3}Mn_{1-x}Cr_xO_3$. *J Appl Phys* 2005;97:103908.
- [16] Hong CS, Hur NH, Choi YN. Magnetic exchange interactions induced by Cr-doping in perovskite manganites. *Solid State Commun* 2005;133:531.
- [17] Roy S, Dubenko IS, Ignatov AY, Ali N, Roy S, Dubenko IS. Study of the colossal magnetoresistance properties of the compound $La_{1-x}Sr_xA_yMn_{1-y}O_3$ ($A = Cr, Re$). *J. Phys Condens Matter* 2000;12:9465.
- [18] Sun Y, Xu X, Zhang Y. Effects of Cr doping in $La_{0.67}Ca_{0.33}MnO_3$: Magnetization, resistivity, and thermopower. *Phys Rev B* 2001;63:054404.
- [19] Sun Y, Tong W, Xu X, Zhang Y. Tuning colossal magnetoresistance response by Cr substitution in $La_{0.67}Sr_{0.33}MnO_3$. *Appl Phys Lett* 2001;78:643.
- [20] Othmani S, Blel R, Bejar M, Sajjedine M, Dhahri E, Hlil EK. New complex magnetic materials for an application in Ericsson refrigerator. *Solid State Commun* 2009;149:969.
- [21] Young RA. The Rietveld method. New York: Oxford University Press; 1993.
- [22] Lacaze AF, Beranger R, Mardion GB, Claudet G, Lacaze AA. Efficiency improvements of a double acting reciprocating magnetic refrigerator. *Cryogenics* 1983;23:427.
- [23] Kallel N, Dhahri J, Zemni S, Dhahri E, Oumezzine M, Ghedira M. Effect, of Cr Doping in $La_{0.7}Sr_{0.3}Mn_{1-x}Cr_xO_3$ with $0 < x < 0.5$. *Phys Status Solidi A* 2001;184(2):319.
- [24] Xavier Jr MM, Cabral FAO, de Araujo JH, Chesman C, Dumelow T. Magnetic and transport properties of polycrystalline $La_{0.7}Sr_{0.3}Mn_{1-x}Fe_xO_3$. *Phys Rev B* 2000;63:012408.
- [25] Rao GH, Sun JR, Kattwinkel A, Haupt L, Baerner K, Schmitt E, Gmelin E. Magnetic, electric and thermal properties of $La_{0.7}Ca_{0.3}Mn_{1-x}Fe_xO_3$ compounds. *Physica B* 1999;269:379.
- [26] Schnelle W, Poddar A, Murugaraj P, Gmelin E, Kremer RK, Sasaki K, Maier J. The effect of annealing conditions on the physical properties of $Nd_{0.67}Sr_{0.33}MnO_{3-\delta}$. *J Phys Condens Matter* 2000;12:4401.